

**Electronic Supplementary Material**

**Crosslinked ether-based polymer for high performance semi-solid  
lithium metal battery via in-situ integration**

Dezhi Yang,<sup>ab</sup> Yanan Yang,<sup>ab</sup> Yeying Cui,<sup>ab</sup> Yiyang Sun<sup>ab</sup> and Tao Zhang<sup>\*abc</sup>

<sup>a</sup> State Key Lab of High Performance Ceramics and Superfine Microstructure, Shanghai Institute of Ceramics, Chinese Academy of Sciences, 1295 Dingxi Road, Shanghai 200050, PR China

<sup>b</sup> Center of Materials Science and Optoelectronics Engineering, University of Chinese Academy of Sciences, Beijing 100049, PR China

<sup>c</sup> Chinese Acad Sci, Shanghai Inst Ceram, CAS Key Lab Mat Energy Convers, Shanghai 201899, PR China

E-mail: taozhang@mail.sic.ac.cn

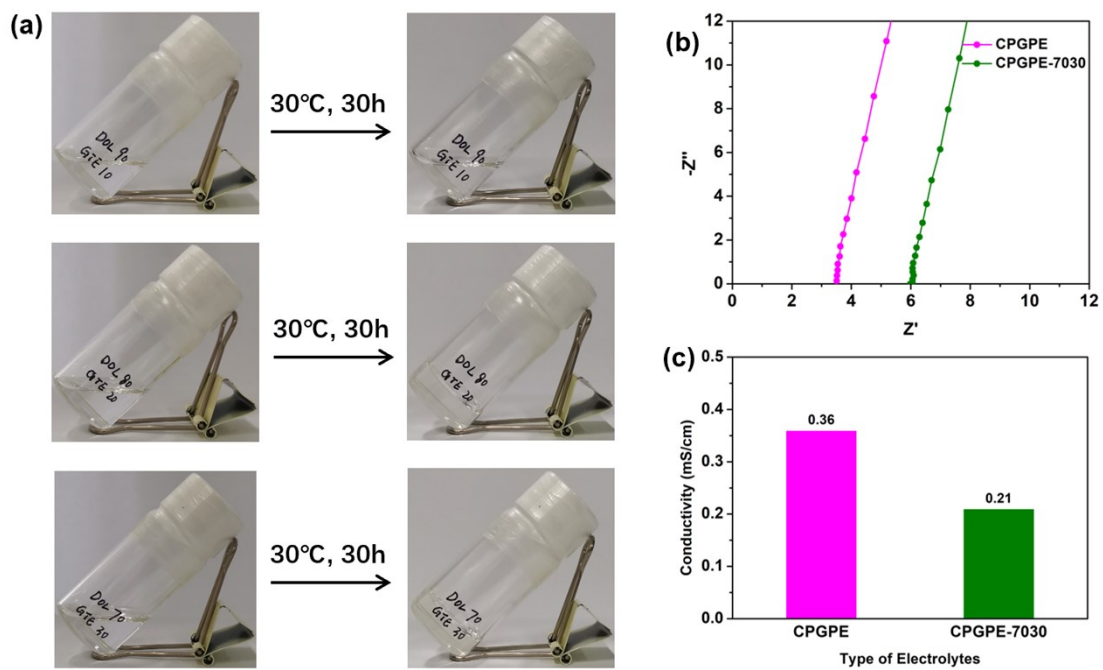


**Fig. S1** (a) Curing situation of different volume ratio between DOL and GTE in the precursor solvent formula of  $5(\text{DOL}(x)\text{-GTE}(100-x)\text{-2HFE-2FEC-1EMC})$ . (b, c) Comparison of the ionic conductivity of different GTE ratio in the electrolyte.

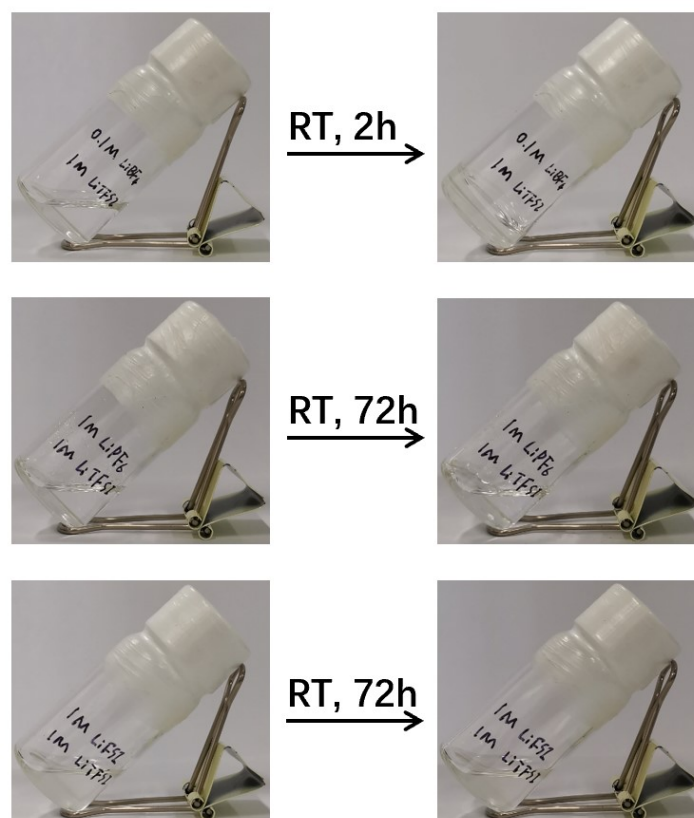


**Fig. S2** Effect of initiators (LiBF<sub>4</sub>, LiPF<sub>6</sub>, and LiFSI) on the crosslinked polymerization of DOL and GTE (80:20, v/v) with 1M LiTFSI.

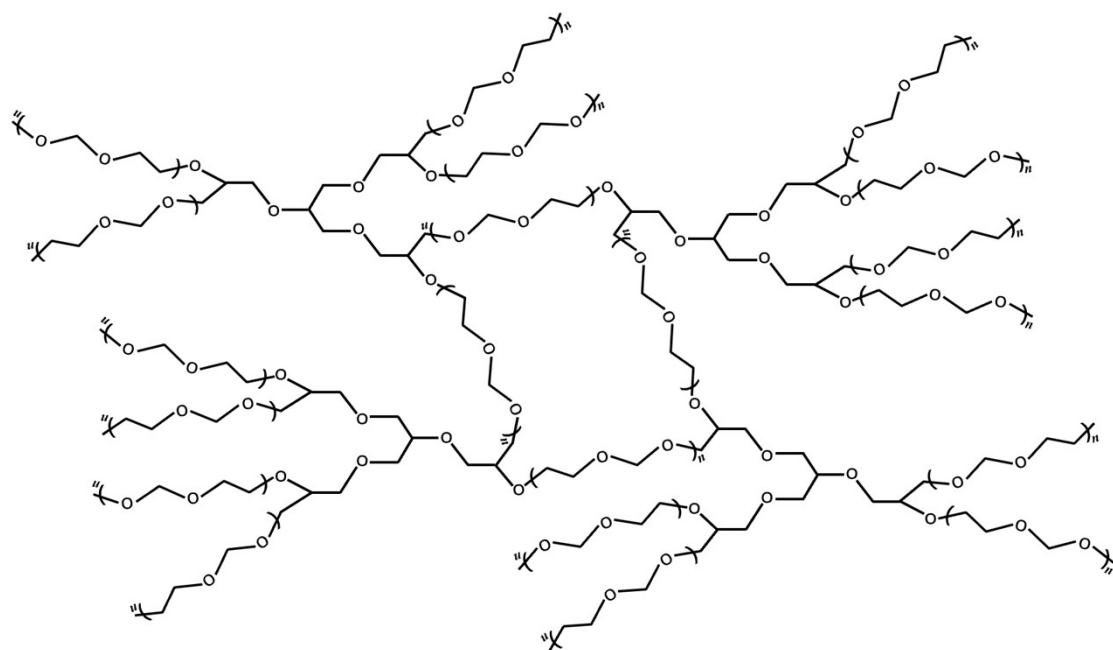


**Fig. S3** The possible polymerization product of DOL and GTE.

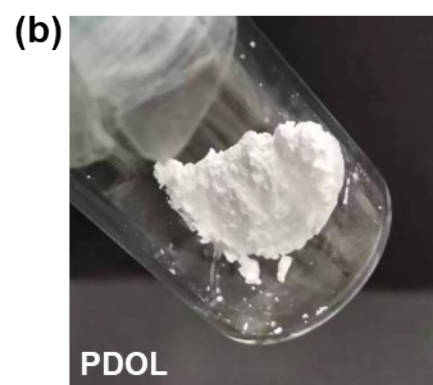
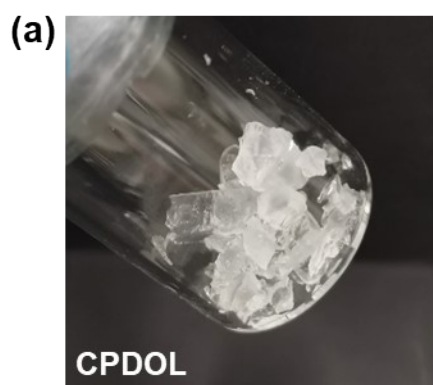


**Fig. S4** Purified polymer obtained from repeated ultrasonic cleaning of (a) CPGPE and (b) PGPE with water and ethanol.

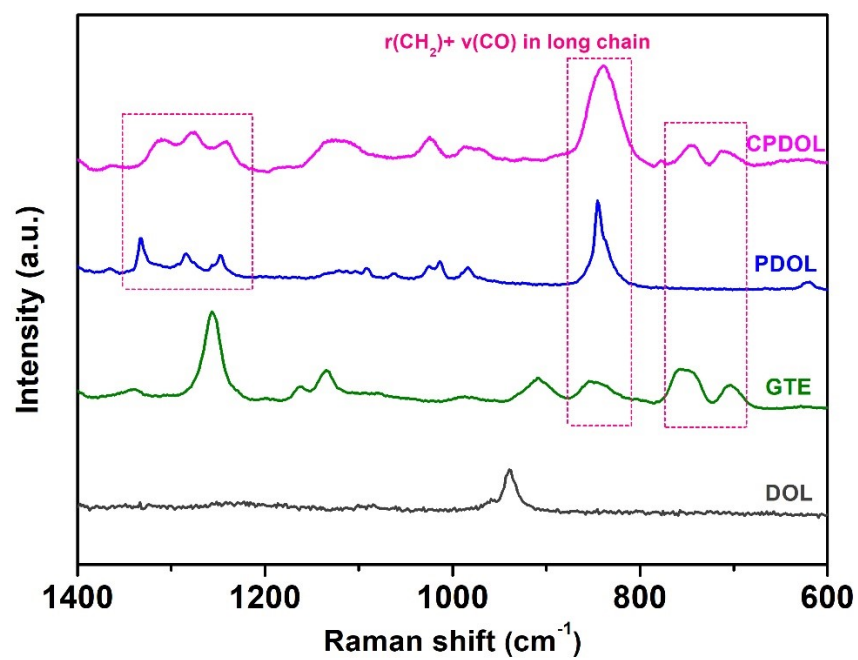
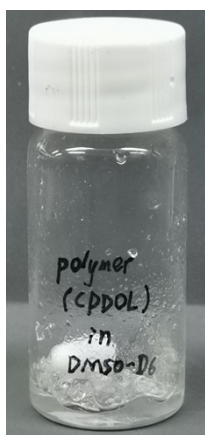
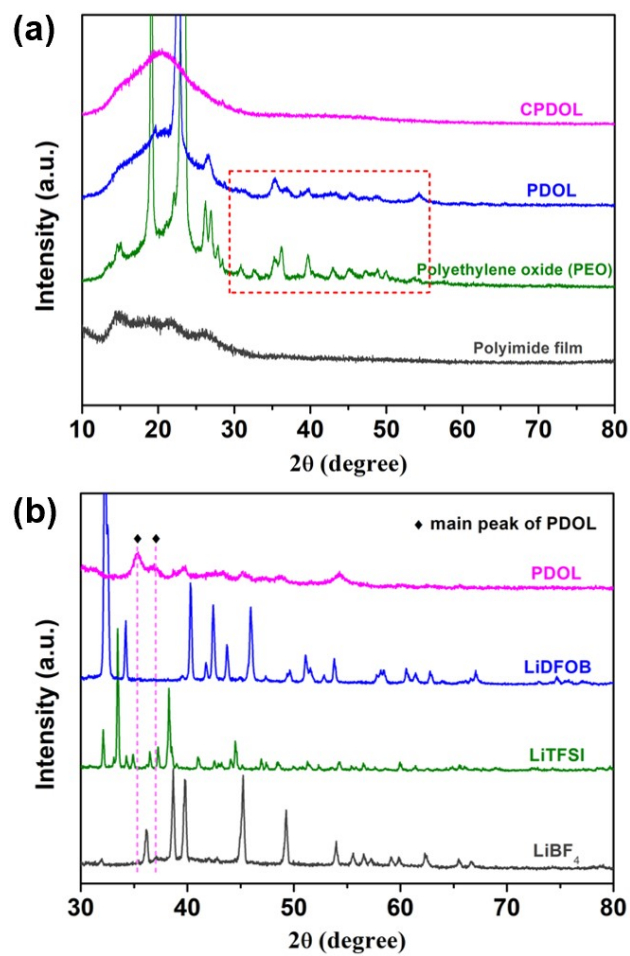


Fig. S5 Raman spectra of DOL, GTE, PDOL, and CPDOL.



**Fig. S6** (a) Optical image of the dissolving state of CPDOL in DMSO-D6.



**Fig. S7** XRD pattern of (a) CPDOL, PDOL, and PEO, (b) PDOL and various lithium salts used in the electrolyte.



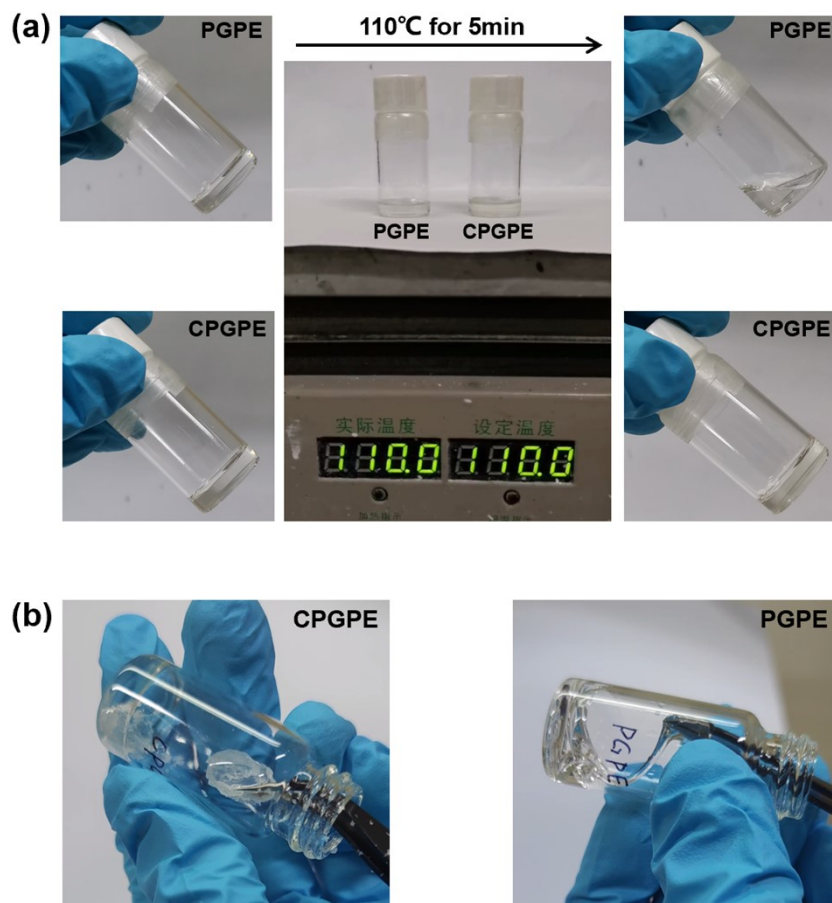


**Fig. S8** (a) Optical images of CPGPE and PGPE before and after heated at 110 °C for 5 minutes. (b) Physical characteristic of CPGPE and PGPE.

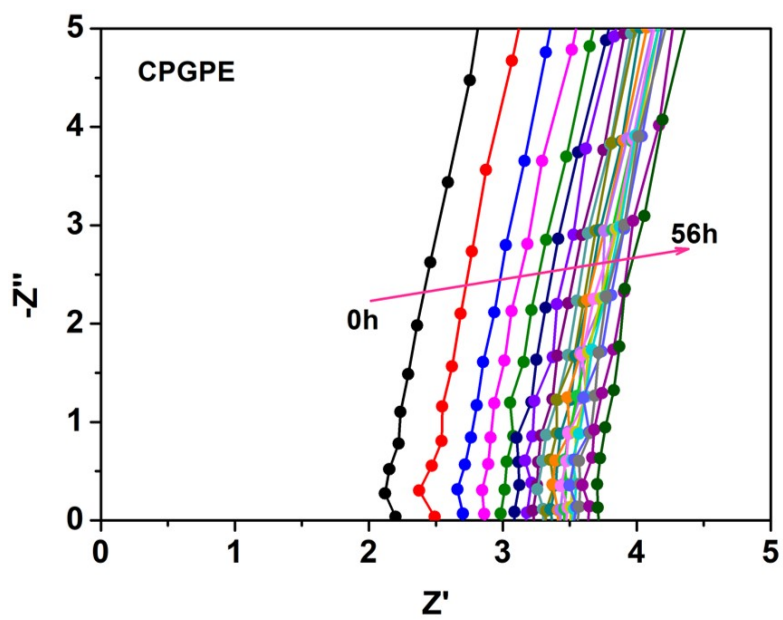


**Fig. S9** Change of EIS plot of the SS|CPGPE|SS cell over time.

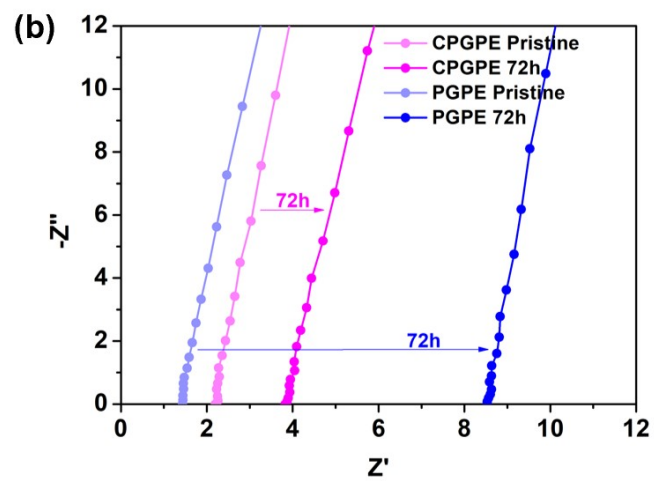
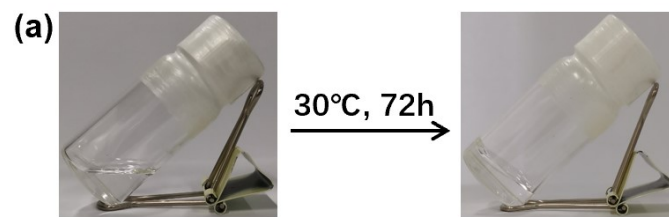
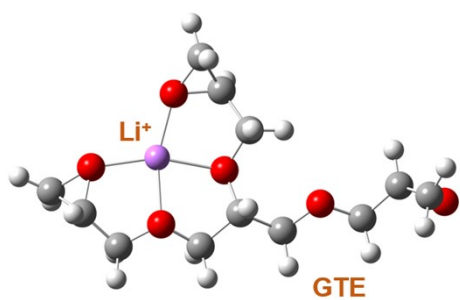
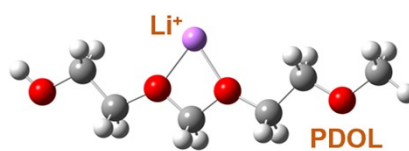


**Fig. S10** (a) Optical image of the curing process of PGPE. (b) Comparison of the EIS plot of SS|CPGPE|SS and SS|PGPE|SS cells before and after solidification.



$E_b = -4.239 \text{ eV}$



$E_b = -2.653 \text{ eV}$

**Fig. S11** (a) Schematic diagram of the interaction of GTE and Li<sup>+</sup>. (b) Schematic diagram of the interaction of PDOL and Li<sup>+</sup>.

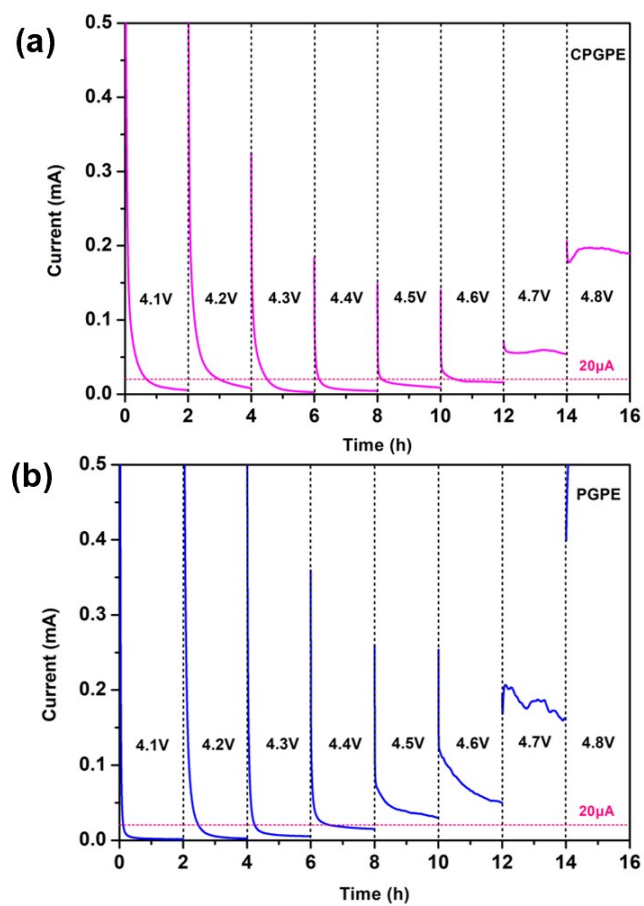


**Fig. S12** Electrochemical floating test of the NCM811|CPGPE|Li and NCM811|PGPE|Li batteries.

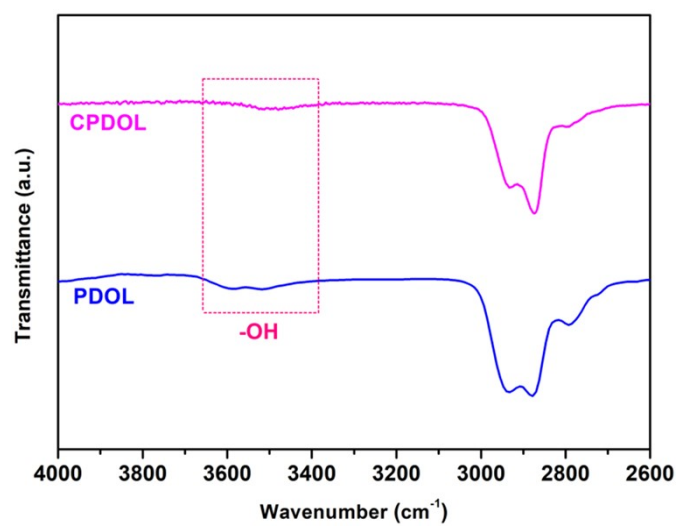


**Fig. S13** Comparison of hydroxyl characteristic peaks of CPDOL and PDOL.

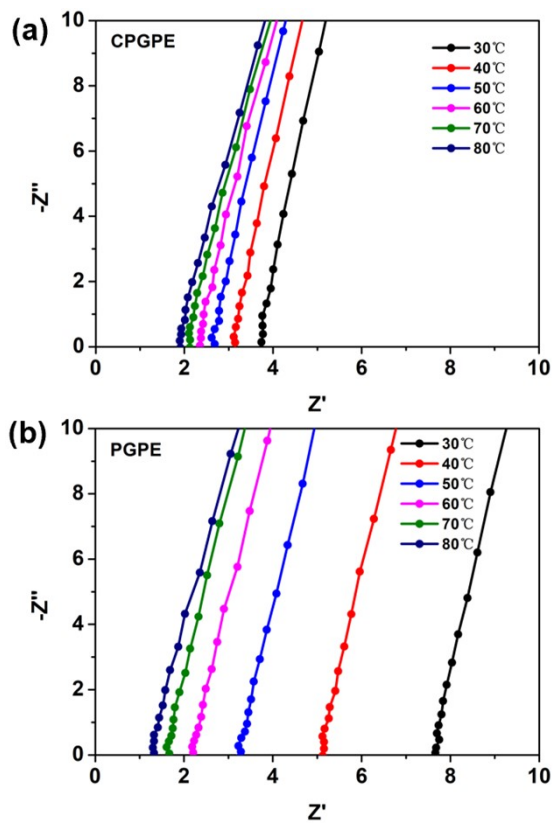


**Fig. S14** Change of EIS plot of the (a) SS|CPGPE|SS and SS|PGPE|SS cells over temperature.

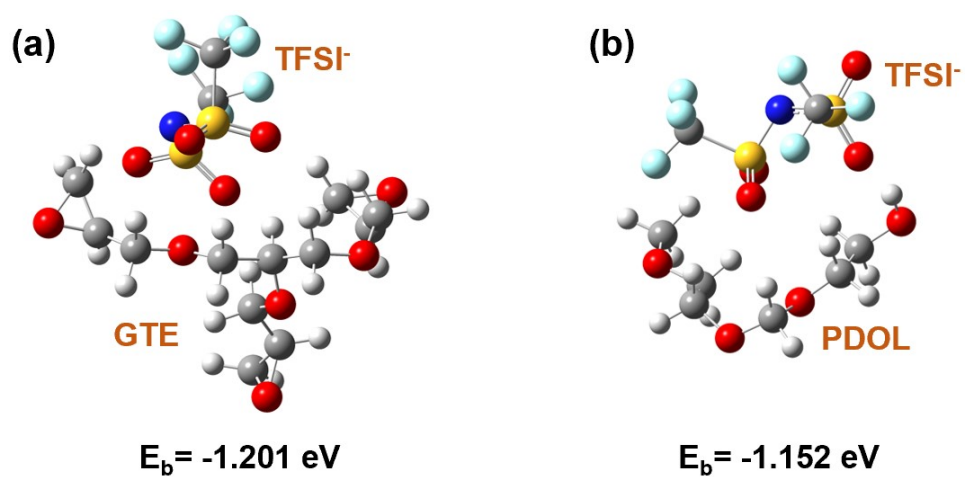


**Fig. S15** (a) Schematic diagram of the interaction of GTE and TFSI<sup>-</sup>. (b) Schematic diagram of the interaction of PDOL and TFSI<sup>-</sup>.



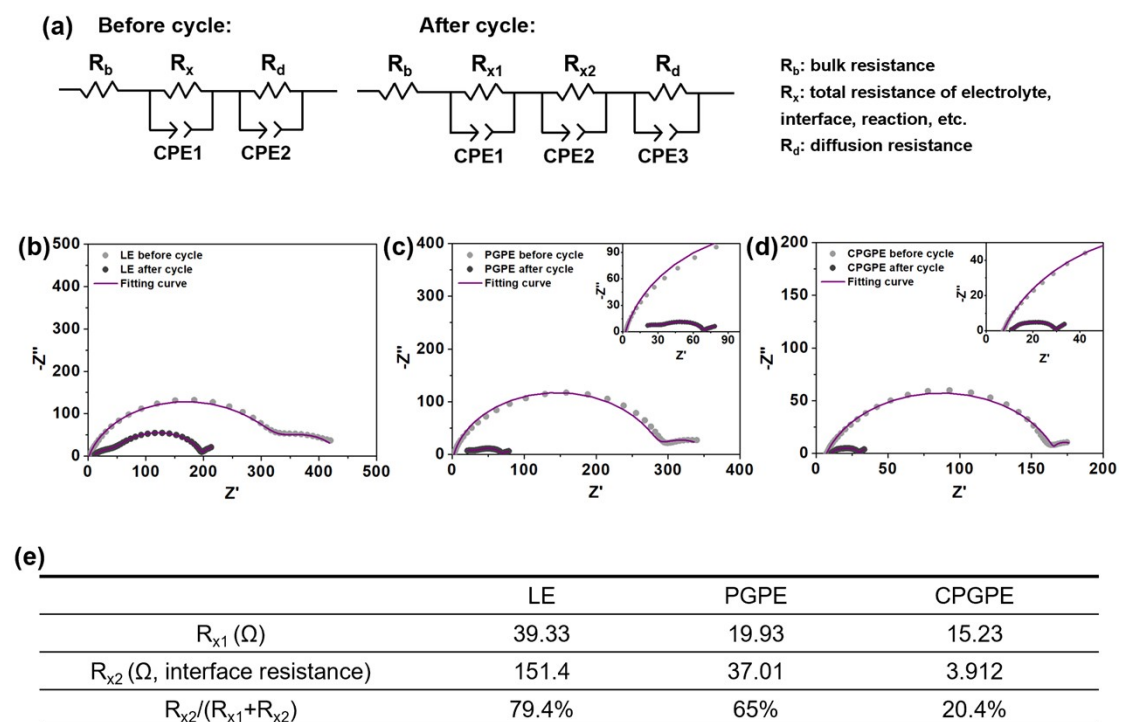


**Fig. S16** (a) Equivalent circuits for the EIS plots of the initial and cycled Li||Li cells. EIS plots and its corresponding fitting curves of the initial and cycled (b) Li|LE|Li cell, (c) Li|PGPE|Li cell, and (d) Li|CPGPE|Li cell. (e) The calculated ratio of interface resistance in the total resistance of mid-frequency region for different types of cycled Li||Li cells.

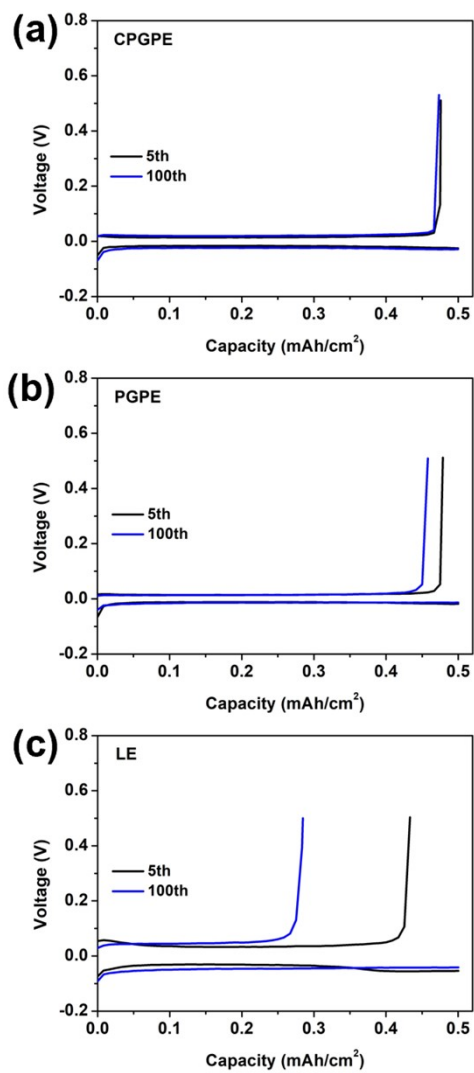


**Fig. S17** Charge/discharge curves of the (a) Li|CPGPE|Cu, (b) Li|PGPE|Cu, and (c) Li|LE|Cu cell at different cycle number.

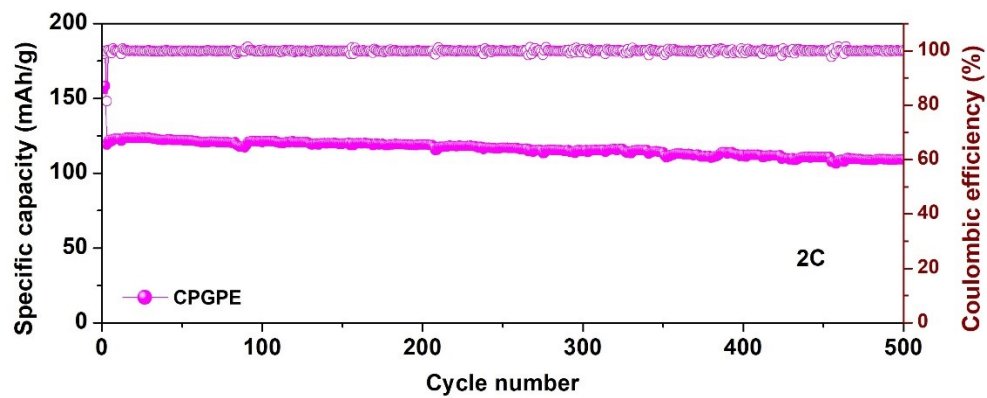


**Fig. S18** Cycling performance of the LFP||Li battery assembled with CPGPE at 2C.

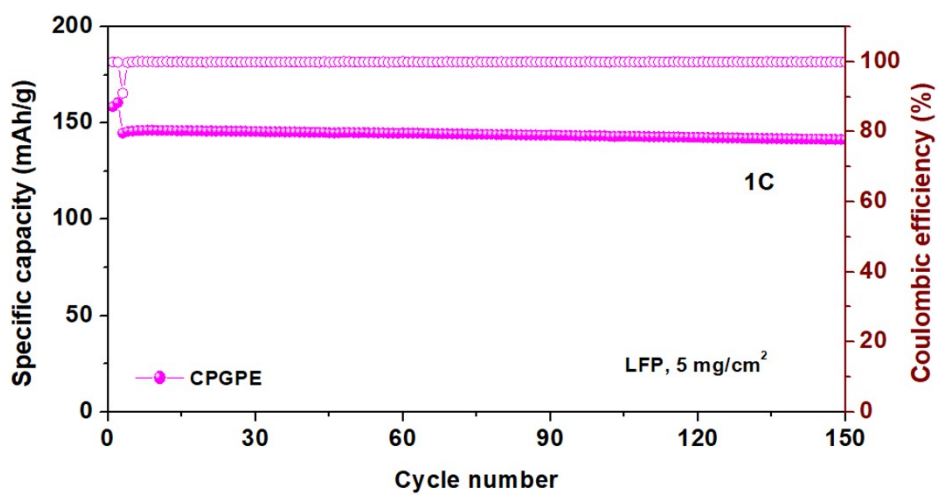


**Fig. S19** Cycling performance of the LFP|CPGPE|Li battery with a high active materials loading of 5 mg/cm<sup>2</sup> at 1C.

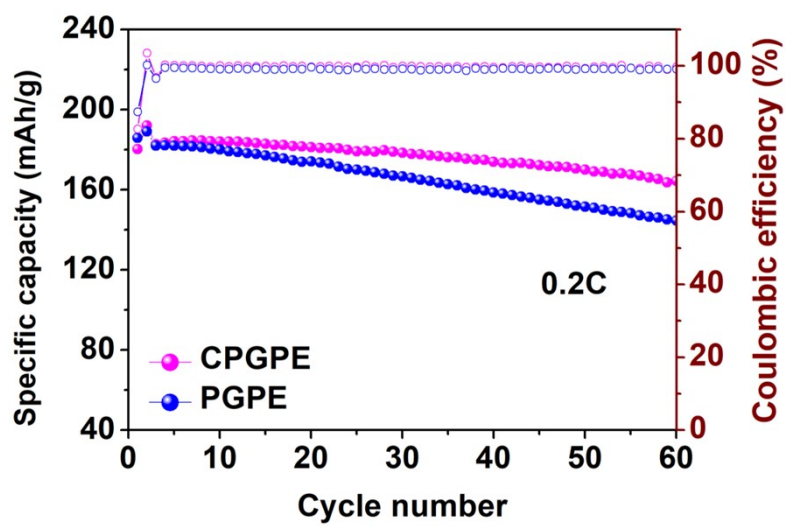


**Fig. S20** Cycling performance of the NCM811||Li batteries assembled with CPGPE and PGPE at 0.2C.

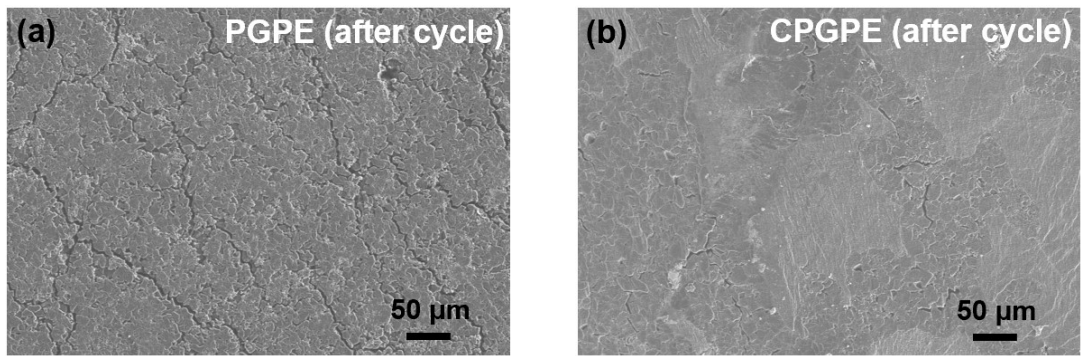


**Fig. S21** SEM images of the lithium anode from the NCM811||Li batteries assembled with (a) PGPE and (b) CPGPE operating for 120 cycles.

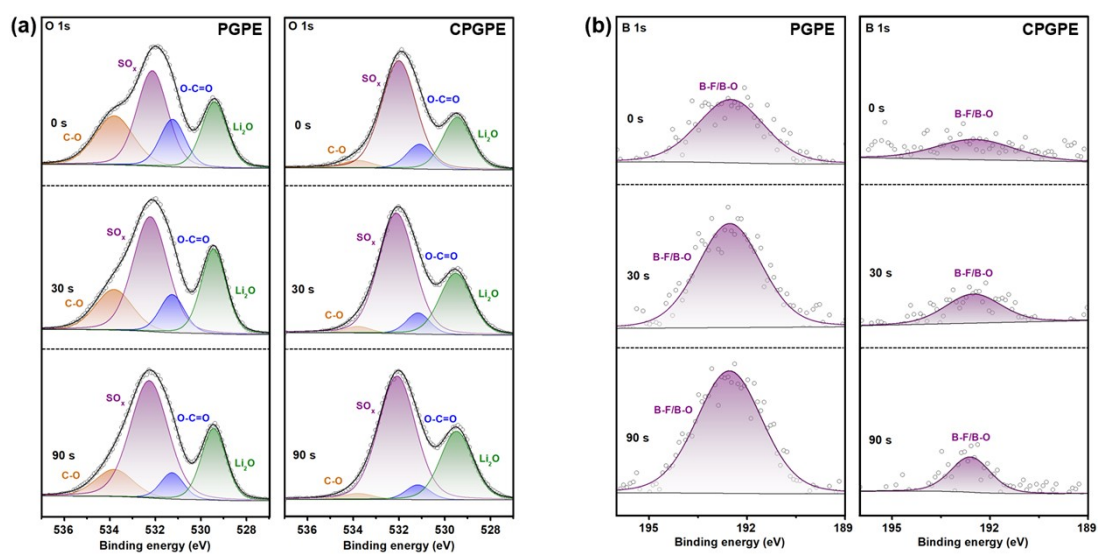


**Fig. S22** XPS (a) O 1s spectra and (b) B 1s spectra of the washed lithium anode from the cycled NCM811||Li battery assembled with CPGPE and PGPE.

**Table S1** A comparison of the electrochemical performance of this work with the similar PDOL based electrolyte in recent years

Electrolyte materials	Physical characteristic	Cathode materials	Active materials loading (mg/cm <sup>2</sup> )	Cycle rate (C)	Cycle number@capacity retention	Ref.
Poly(DOL-TTE)	All-solid	LFP	-	0.2	200cycle@80%	1
PTADOL	All-solid	LFP	3	0.5	300cycle@85.6%	2
		NCM811	3	0.5	150cycle@81.4%	
PSiDOL	All-solid	LFP	2.5	0.5	160cycle@97%	3
		NCM811		0.3	100cycle@90%	
PDOL/SN/FEC	Gel	NCM811	3	1	100cycle@70.59%	4
PDOL/SN	Gel	LFP	2	1	1000cycle@83.55%	5
KMSP@PDOL/DME	Gel	LFP	2.5	1	500cycle@90.3%	6
PDOL/DME/FEC	Gel	LFP	4	0.5	200cycle@~90%	7
				2	1000cycle@77.6%	
PDOL/DOL	Gel	LFP	4.2	1	500cycle@69.28%	8
PDOL/DME	Gel	LFP	10	1	700cycle@~60%	9
PDOL/DOL/LiNO <sub>3</sub>	Gel	LFP	3	0.5	450cycle@72.74(50°C)	10
				2	500cycle@76.9%	
PDOL/DOL/PDA/PVDF-HFP	Gel	LFP	2.2	1	200cycle@87.13%	11
				2	800cycle@83.2%	
<b>This work</b>	<b>Gel</b>	<b>LFP</b>	<b>2</b>	<b>1</b>	<b>1000cycle@88%</b>	
		<b>LFP</b>	<b>2</b>	<b>2</b>	<b>500cycle@91.7%</b>	
		<b>NCM811</b>	<b>2.5</b>	<b>0.5</b>	<b>165cycle@80.2%</b>	



## References

1. S. Wen, C. Luo, Q. Wang, Z. Wei, Y. Zeng, Y. Jiang, G. Zhang, H. Xu, J. Wang, C. Wang, J. Chang and Y. Deng, *Energy Storage Materials*, 2022, **47**, 453-461.
2. Y. Du, L. Zhao, C. Xiong, Z. Sun, S. Liu, C. Li, S. Hao, W. Zhou and H. Li, *Energy Storage Materials*, 2023, **56**, 310-318.
3. J. Cui, Y. Du, L. Zhao, X. Li, Z. Sun, D. Li and H. Li, *Chemical Engineering Journal*, 2023, **461**.
4. Y. Liu and Y. Xu, *Chemical Engineering Journal*, 2022, **433**.
5. Q. Liu, B. Cai, S. Li, Q. Yu, F. Lv, F. Kang, Q. Wang and B. Li, *Journal of Materials Chemistry A*, 2020, **8**, 7197-7204.
6. D. Chen, T. Zhu, M. Zhu, S. Yuan, P. Kang, W. Cui, J. Lan, X. Yang and G. Sui, *Energy Storage Materials*, 2022, **53**, 937-945.
7. X. Jiao, J. Wang, G. Gao, X. Zhang, C. Fu, L. Wang, Y. Wang and T. Liu, *ACS Applied Materials & Interfaces*, 2021, **13**, 60054-60062.
8. H. Cheng, J. Zhu, H. Jin, C. Gao, H. Liu, N. Cai, Y. Liu, P. Zhang and M. Wang, *Materials Today Energy*, 2021, **20**.
9. J. Zheng, W. Zhang, C. Huang, Z. Shen, X. Wang, J. Guo, S. Li, S. Mao and Y. Lu, *Materials Today Energy*, 2022, **26**.
10. Q. Wang, Y. Ma, Y. Wang, X. He, D. Zhang, Z. Li, H. Sun, Q. Sun, B. Wang and L.-Z. Fan, *Chemical Engineering Journal*, 2024, **484**.
11. D. Chen, M. Zhu, P. Kang, T. Zhu, H. Yuan, J. Lan, X. Yang and G. Sui, *Advanced Science*, 2021, **9**.